# First Performance Results of Ce:GAGG Scintillation Crystals With Silicon Photomultipliers

Jung Yeol Yeom, *Member, IEEE*, Seiichi Yamamoto, *Member, IEEE*, Stephen E. Derenzo, *Fellow, IEEE*, Virginia Ch. Spanoudaki, Kei Kamada, Takanori Endo, and Craig S. Levin, *Member, IEEE*

***Abstract*—A new single-crystal Cerium doped $Gd_3Al_2Ga_3O_{12}$ (GAGG) scintillation crystal with high luminosity, high density and relatively fast decay time has successfully been grown. We report on the first performance results of the new GAGG scintillation crystal read out with silicon photomultipliers (SiPM) from Hamamatsu (MPPC) and FBK. The best energy resolution (511 keV peak of Ge-68) of 7.9% was attained with GAGG coupled to MPPC and 9.0% with the FBK SiPM after correcting for non-linearity. On the other hand, the best coincidence resolving time (FWHM) of polished $3 \times 3 \times 5\ mm^3$ and $3 \times 3 \times 20\ mm^3$ crystals were $464 \pm 12$ ps and $577 \pm 22$ ps for GAGG crystals compared to $179 \pm 8$ ps and $214 \pm 6$ ps for LYSO crystals respectively with MPPCs. The rise time of GAGG was measured to be 200 ps (75%) and 6 ns (25%) while the decay time was 140 ns (92%), 500 ns (7.7%) 6000 ns (0.3%).**

***Index Terms*—Ce:GAGG, gamma-ray spectroscopy, PET, scintillators, silicon photomultipliers, SPECT.**

TABLE I
PHYSICAL AND SCINTILLATION PROPERTIES OF GAGG

| Scintillator | Ce:GAGG | LYSO:Ce[2] | BGO | CsI:Tl |
|---|---|---|---|---|
| Density (g/cm$^3$) | 6.63[1] | 7.1 | 7.1 | 4.5 |
| Light yield (ph/Mev) | 46,000 | 32,000 | 9,000 | 60,000 |
| Decay time (ns) | 90 | 41 | 300 | 1000 |
| Peak Emission (nm) | 520 | 420 | 480 | 545 |
| Energy resolution (% @ 662 keV) | 4.9% | 8 | 12 | 5% |

[1] Theoretical value
[2] Values from Saint-Gobain Ceramics & Plastics, Inc.

## I. INTRODUCTION

A wide range of scintillators are available for the detection of ionizing radiation of which a handful is suitable for use in nuclear medicine, i.e., Position Emission Tomography (PET) and Single Photon Emission Computed Tomography (SPECT) [1]–[3]. An ideal scintillator for PET would have high luminosity, high density and effective atomic number, fast rise and decay time constants, a peak emission wavelength that matches well with the spectral sensitivity of the photodetector and low non-proportionality. In addition, the scintillation material should be inexpensive to manufacture, non-hygroscopic, rugged and preferably produce no intrinsic radiation. At the present, Lutetium based oxide scintillation crystals like cerium doped lutetium oxyorthosilicate (LSO), lutetium-yttrium oxyorthosilicate (LYSO) and lutetium gadolinium oxyorthosilicate (LGSO) are most commonly used in commercial PET systems as they offer the best tradeoffs of the aforementioned factors [4]–[6].

Ceramic Gadolinium Garnet based scintillators also feature high luminosity, high density and relatively fast decay time [7]. This family of scintillators include the cerium doped $(Gd, Y)_3(Al, Ga)_5O_{12}$ (GYGAG) scintillator that was reported to show good performance for gamma spectroscopy [8].

Recently, a new single-crystal Cerium doped $Gd_3\ Al_2Ga_3O_{12}$ (GAGG) crystal has successfully been grown using Czochraski method [9], paving the way for the production of large and high quality single-crystal ingots. The GAGG scintillator, compared to GYGAG as mentioned above, has the inherent advantage of a higher density and effective atomic number due to the absence of Yttrium atoms, making it an attractive candidate for applications such as PET and gamma spectroscopy where higher energy radiation has to be detected. The properties of GAGG scintillation crystal as reported in [9] and typical values of common scintillators have been summarized in Table I.

A photodetector is often used in conjunction with scintillators to convert light photons emitted by the scintillator upon interaction with radiation to electrical signals. The silicon photomultiplier (SiPM), is a relatively new semiconductor photode-

Manuscript received June 16, 2012; revised November 12, 2012; accepted December 06, 2012. Date of publication February 01, 2013; date of current version April 10, 2013. This work was supported in part by the Stanford Dean's Postdoctoral Fellowship, Cygnus Fellowship, the AXA Research Fund and in part by the Department of Homeland Security, Domestic Nuclear Detection Office (DHS/DNDO).

J. Y. Yeom is with the Molecular Imaging Program at Stanford and Department of Radiology, Stanford University, Stanford, CA 94305, USA (e-mail: yeomjy@stanford.edu).

S. Yamamoto is with the Department of Radiological and Medical Laboratory Sciences, Nagoya University, Nagoya 461-8673, Japan (e-mail: s-yama@met.nagoya-u.ac.jp).

S. E. Derenzo is with the Department of Radiotracer Development and Imaging Technology, Lawrence Berkeley National Laboratory, Berkeley, CA 94720, USA (e-mail: sederenzo@lbl.gov).

V. C. Spanoudaki is with the Molecular Imaging Program at Stanford and Department of Radiology, Stanford University Stanford, CA 94305, USA. She is now with Koch Institute for Integrative Cancer Research, MIT, MA 02139, USA (e-mail: vspan@mit.edu).

K. Kamada and T. Endo are with the Materials Research Laboratory, Furukawa Co. Ltd., Tsukuba 305-0856, Japan (e-mail: {k-kamada, ta-endou}@furukawakk.co.jp).

C. S. Levin is with the Departments of Radiology, Physics and Electrical Engineering, Stanford University, Stanford, CA 94305, USA (e-mail: cslevin@stanford.edu).

Color versions of one or more of the figures in this paper are available online at http://ieeexplore.ieee.org.

Digital Object Identifier 10.1109/TNS.2012.2233497

0018-9499/$31.00 © 2013 IEEE

Authorized licensed use limited to: Australian National University. Downloaded on March 12,2020 at 00:31:51 UTC from IEEE Xplore. Restrictions apply.

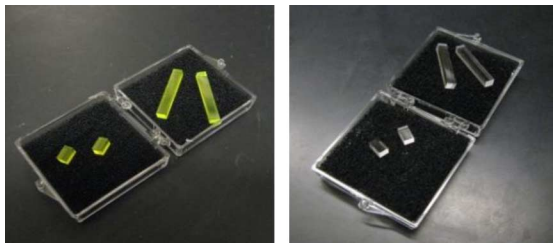

Fig. 1. Picture of the GAGG (left) and LYSO samples. The GAGG crystal is yellow in color (refer to electronic version for color).

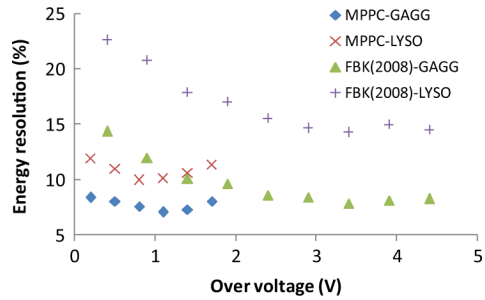


Fig. 2. Energy resolution (not corrected for saturation) of GAGG and LYSO with MPPC and FBK SiPM. The energy resolution increases with overvoltage due to an increase in gain and PDE but degrades when the effect of dark counts and excess noise exceeds the signal improvement.

tector, with properties such as high gain and quantum efficiency (but lower fill factor), fast response, compactness and insensitivity to magnetic fields. Despite suffering from crosstalk, afterpulsing and dark counts that increase with bias voltage and a nonlinear output at high photon numbers, they are finding increasing applications in fields like particle physics experiments, PET, biomedical research, space exploration, etc [10]–[13].

In this paper, we present the first performance results of the new GAGG scintillation crystal read out with SiPMs, with focus on nuclear medicine applications, and results are compared with that of LYSO scintillators.

## II. Experimental Setup, Methods and Results

### A. Materials Description

In this study, the performances and characteristics of polished $3 \times 3 \times 5\ \mathrm{mm}^3$ and $3 \times 3 \times 20\ \mathrm{mm}^3$ GAGG scintillators (Furukawa Co. Ltd.) are assessed in comparison with same sized LYSO crystals (Agile Technologies, Inc.) (Fig. 1). The shorter crystals would provide timing performance of the detector without light propagation effects within the crystal [14] while the longer 20 mm crystals, typical scintillator thickness in PET to effectively stop the 511 keV annihilation photons, are used to assess the timing performance that these crystals can achieve when integrated into PET scanners. The 5 mm long crystals have been wrapped with Teflon tape while 3M ESR film (Vikuiti) has been used as reflector for the 20 mm crystals. The reflectors (i.e., diffused or specular) have been chosen as it has been shown to give better timing performance for their respective crystal dimensions [15].

Two types of SiPMs have been selected for this study. One is a Hamamatsu Multi-Pixel Photon Counter (MPPC, $3 \times 3\ \mathrm{mm}^2$ active area, $50\ \mu\mathrm{m}$ pixel, model no: S10362-33) with a peak spectral sensitivity at around 440 nm which matches closely with the peak emission wavelength of the LYSO crystals, while the second SiPM is a prototype (year 2008) of FBK ($3 \times 3\ \mathrm{mm}^2$ active area, $50\ \mu\mathrm{m}$ pixel) with a peak spectral sensitivity at around 530 nm that coincides almost exactly with GAGG.

Two light tight detector holders with sockets for the pins of the SiPM have been fabricated. A bias-tee through which the bias voltages to the SiPM is supplied and ac signals are transmitted is included in each holder. Each crystal has been coupled to the SiPM with optical grease (Bicron BC-630). The holder, bias tee circuitry, SiPM and scintillation crystal form a detector module.

### B. Energy Resolution

The energy resolution was evaluated with a Ge-68 radiation source by reading out the detector module (5 mm long crystals) with a Cremat CR112 charge sensitive amplifier (CSA) and filtering with an ORTEC 674 spectroscopy amplifier at $2\ \mu\mathrm{s}$ shaping time constant. The output was fed to a high speed oscilloscope (Agilent DSO90254A) to histogram the peak energies, and a Gaussian fit was carried out on the annihilation photon peak offline.

The energy resolutions measured with the setup explained above is shown in Fig. 2. The GAGG crystal, with a higher light output, produced better energy resolutions of 7.1% with MPPC at 1.1 V overvoltage (ov) and 7.9% with FBK SiPM (3.3 V ov) compared to LYSO-10.1% (0.8 V ov) and 14.3% (3.3 V ov) with MPPC and FBK SiPM respectively.

It should be noted that although FBK devices have a peak spectral sensitivity that matches better with GAGG, the MPPC still has higher photon detection efficiency (PDE) at both GAGG and LYSO emission wavelength, leading to the better energy resolutions with MPPC devices. On a related matter, although the luminosity of GAGG is about 1.5 times brighter than LYSO, the ratio of GAGG to LYSO output signal amplitude (511 keV full energy peak) was measured to be $\sim 1.2$ with MPPC while the ratio was $\sim 1.8$ with FBK SiPM, clearly reflecting the maximum spectral sensitivity match of each device with the crystals.

In SiPMs, the output is proportional to the number of fired microcells, leading to a saturation effect associated with the finite number of microcells present. This effect and, to a smaller extend, crosstalk and afterpulsing also contributes to the nonlinear output of SiPM [16], giving an artificially good energy resolution at high photon flux and bias voltages. The former dominant effect can be corrected by plotting a non-linearity curve (pulse height distributions) of known sources and fitting with the equation below, solving for the unknowns ($a$ and $b$) and compensating for the saturated energy spectrum [17].

$$y = a(1 - e^{-bx}) \tag{1}$$

where $y = \mathrm{output}$ voltage and $x = \mathrm{energy}$ of photon.

The non-linearity (saturation) has been assessed using 5 mm long GAGG crystal. The centroid values of each energy peak of Ba-133 (81 keV, 356 keV), Ge-68 (511 keV) and Cs-137 (662

Authorized licensed use limited to: Australian National University. Downloaded on March 12,2020 at 00:31:51 UTC from IEEE Xplore. Restrictions apply.

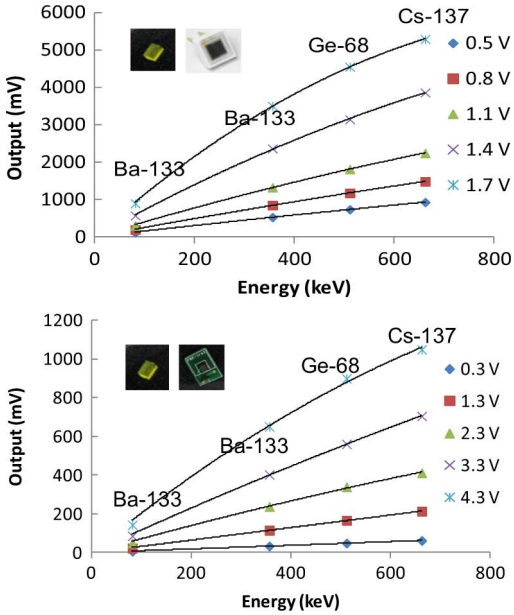


Fig. 3. Linearity curves of GAGG crystal when coupled to MPPC (top) and FBK SiPM (bottom).

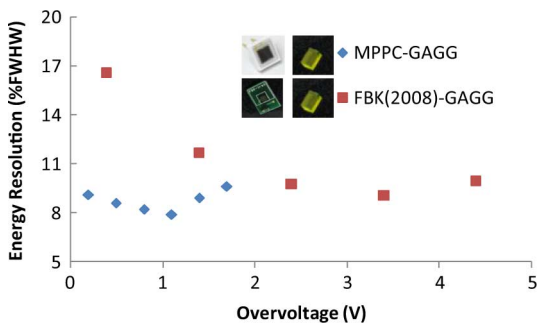


Fig. 4. Saturation corrected energy resolution of GAGG crystal.

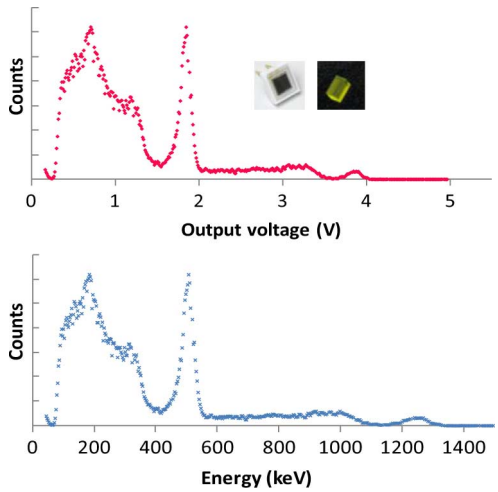


Fig. 5. Distribution of pulse height of a Na-22 source with GAGG-MPPC at 1.1 V overvoltage before correction (top) and distribution of energy after correcting for the saturation shown in Fig. 3 (bottom).

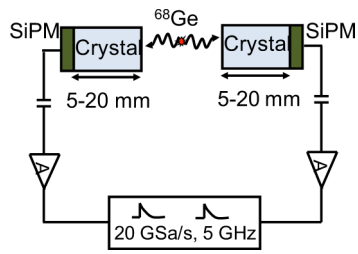


Fig. 6. Setup for the CRT measurements.

keV) sources have been plotted for various bias voltages and are shown in Fig. 3.

Using these curves, the energy spectrum at each bias voltage can be corrected and a more accurate energy resolution can be calculated. The corrected energy resolution of the 511 keV full energy annihilation photon peak for GAGG crystals coupled to MPPC and FBK SiPM is shown in Fig. 4. The best energy resolutions of GAGG crystal following non-linearity corrections degrade from 7.1% to 7.9% with MPPC and 7.9% to 9.0% for FBK SiPM. In Fig. 5, the energy spectrum of a Na-22 source before and after correction is shown when detected with GAGG-MPPC. After correction, it can be seen the position of the 1.275 MeV peak is located properly relative to the position of the 511 keV annihilation peak.

### C. Timing Resolution

The setup for evaluating the timing performance of the crystals is illustrated in Fig. 6. The coincidence resolving time (CRT) was obtained using a Ge-68 source placed between two head-on detector modules with identical crystal and SiPM types. Each SiPM was read out with a high speed RF transimpedance amplifier (Minicircuits Mar $-3$SM+) and leading edge triggering was performed with the scope. The time differences between the two modules (performed with scope) were saved offline and the timing resolution was calculated by Gaussian fitting. No other algorithms or filtering to reduce the effect of dark counts or improve timing were performed.

The CRTs are summarized in Fig. 7. For all similar sized crystals, MPPC showed better timing performances. With 5 mm long crystals, LYSO produced a CRT (FWHM) of $179 \pm 8$ ps (1.9 V ov), while the GAGG produced a timing resolution of $464 \pm 12$ ps (1.7 V ov). These values degraded to $242 \pm 10$ ps (4.5 V ov) and $524 \pm 24$ ps (4.5 V ov) respectively with FBK SiPM. With a more PET system relevant 20 mm long crystal coupled to MPPC, we obtained a timing resolution $214 \pm 6$ ps (1.7 V ov) and $577 \pm 22$ ps (1.7 V ov) for LYSO and GAGG respectively.

### D. Rise and Decay Time

The timing resolution of a signal is inversely proportional to the slope of the leading edge of a pulse when it crosses the trigger threshold [18], which is heavily dependent on the crystal rise and decay time [14], [19].

To investigate the factors leading to the poor timing performance of GAGG, the rise and decay time of a $3 \times 3 \times 10$ mm$^3$ GAGG sample, painted black on five faces to reduce reflections and laid on its long side to reduce propagation time within the crystal, have been assessed. The setup for this measurement is explained in [20], [21] and the arrival time spectrum determination is based on the delayed coincidence method [22]. The

Authorized licensed use limited to: Australian National University. Downloaded on March 12,2020 at 00:31:51 UTC from IEEE Xplore. Restrictions apply.

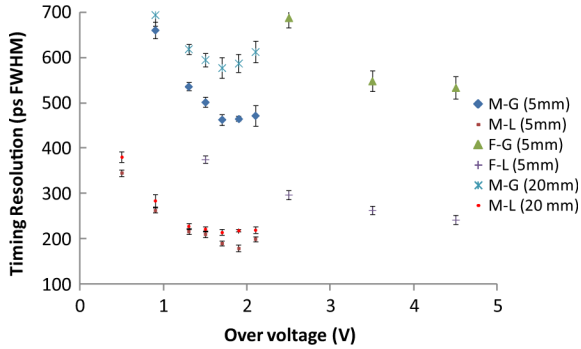


Fig. 7. CRT for GAGG and LYSO coupled to MPPC and FBK SiPM. The error bar is the standard deviation of 5 measurements, each measurement comprising of 1000 coincident events.

unpainted $3\ \mathrm{mm} \times 10\ \mathrm{mm}$ side was excited by pulsed X-ray beam (18 keV average energy) at an incident angle of 45 degrees from the crystal surface. Scintillation light from the same surface was recorded from 90 degrees from the irradiated X-ray beam direction and 45 degrees from the crystal surface.

The measurement taken with 1.5 MHz X-ray pulse repetition rate is shown in Fig. 8. Most of the scintillation was found to have a fast initial rise (initial intensity 75%), consistent with prompt carrier trapping on the $Ce^{3+}$. The rise time of this component was 0.2 ns. However, this value also includes the propagation time within the 3 mm thick crystal and a thinner crystal would probably give a faster rise time. Some of the scintillation output had a 6 ns rise time (initial intensity 25%), consistent with initial $Gd^{3+}$ excitation and transfer to the $Ce^{3+}$ that occur because the excited states of $Gd^{3+}$ ion overlap the absorption bands of $Ce^{3+}$[23]. The primary exponential decay time was 140 ns (92% of the light). We also ran pulsed X-ray at 10 times slower rate (150 kHz) to fit to the slower components and these were 500 ns (7.7%) and 6000 ns (0.3%).

## III. Discussion

The energy resolution presented in this paper was obtained using a Gaussian fit to the full energy peak. If the background was included into the fitting function, e.g., with a exponential and constant term, the energy resolution will likely be slightly lower. It should also be noted that the FBK SiPMs used in this study are earlier prototypes (2008) and that there are newer devices with improved performances [24], [25].

As expected, the much higher light output of GAGG compared to LYSO crystals lead to a better energy resolution. It should be stressed that although FBK SiPM was selected for their spectral sensitivity (wavelength) match with GAGG, the two SiPM structures (P-on-N for MPPC and N-on-P for FBK SiPM) are inherently different [26] with the P-on-N type SiPM (MPPC) having a higher quantum efficiency across the emission wavelength of both crystals [27], [28].

The non-linearity correction explained in Section II is a straightforward way to compensate for saturation but this method does not take into account the cross-talk and afterpulsing that occur in the SiPM, which can be significant at

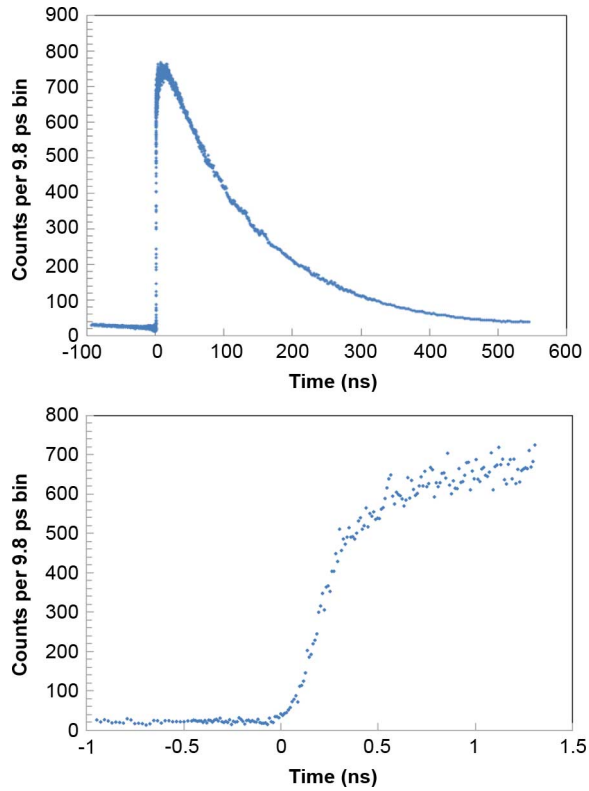


Fig. 8. Pulsed X-ray time response of GAGG 3 mm thick crystal (top) and close up of the rise time of photon arrival time distribution (bottom).

high bias voltages. Under severely saturated conditions like at higher bias voltages or larger radiation energies, this method can be less accurate as the exponential fitting function can magnify a small error in the dependent variable ($y$ of (1)) to produce a large fluctuation in the dependent variable ($x$ of (1)). For a more comprehensive approach, methods like modeling of the SiPM response can be applied [29].

For timing resolution measurements, although the values obtained may be improved further, for example by applying filters and algorithms to reduce the effect of dark counts, they have not been applied in this study to omit dependence on these methods [25], [30]. From Fig. 6, better timing resolutions was obtained with MPPC compared to FBK SiPM due to the difference of PDE in of the two devices, as expected. However, the CRT of GAGG was far poorer than that of LYSO, which was not anticipated. The light output of GAGG is about 1.5 times higher and the decay time is about 2.2 times slower than LYSO according to the data given in [9]. Thus theoretically, assuming the same PDE, we would expect a CRT degradation of about only 1.5 times.

The reason for this has been elucidated through the rise/decay time measurement of the crystal. The rise time, measured for the first time, had a second slow component which partly degrades the timing resolution of the crystal. More importantly, we found that the decay time was also slower than has been reported. This may be due to the samples tested or differences in measurement setup and methods between the two studies but the results presented here agree better with our timing resolution data.

Authorized licensed use limited to: Australian National University. Downloaded on March 12,2020 at 00:31:51 UTC from IEEE Xplore. Restrictions apply.

## IV. Summary and Conclusion

The Ce:GAGG scintillation crystal is a bright and relatively fast scintillator that gives good energy resolution but poorer timing performance compared to the widely used LYSO scintillator.

For PET applications, GAGG is superior to BGO in most areas except for stopping power and can be expected to produce better images, but at a price of higher manufacturing cost associated with higher raw materials cost and smaller ingot size. On the other hand, GAGG, compared to LYSO and LSO, despite having a better energy resolution, is inferior in terms of more crucial properties such as stopping power and timing resolution. However, the two main raw materials for GAGG—gadolinium oxide and gallium oxide—have traditionally been less costly compared to lutetium oxide. It is thus expected that GAGG can be manufactured at a lower cost compared to lutetium based scintillation crystals.

As GAGG has no intrinsic radioactivity and due to its superior energy resolution, it is suitable for gamma-ray spectroscopy and imaging under conditions that necessitates a faster decay time than scintillators like CsI(Tl). The higher light output would also allow higher spatial resolution block detectors designs for SPECT and PET applications due to the higher signals produced with GAGG [31].

## Acknowledgment

The authors would like to thank S. M. Hanrahan of Lawrence Berkeley National Laboratory for carrying out the pulsed X-ray measurements.

## References

[1] W. W. Moses, "Scintillator requirements for medical imaging," in *Proc. Int. Conf. on Inorganic Scintillators and Their Applicat.: SCINT99*, Moscow, Russia, 1999, pp. 11–21.

[2] L. Melcher, "Perspectives on future development of new scintillators," *Nucl. Instrum. Meth. A.*, vol. 537, pp. 6–14, Jan. 2005.

[3] C. W. E. Van Eijk, "Radiation detector developments in medical applications: Inorganic scintillators in positron emission tomography," *Rad. Protect. Dosim.*, vol. 129, no. 1–3, pp. 13–21, 2008.

[4] C. Melcher and J. S. Schweitzer, "Cerium-doped lutetium oxyorthosilicate: A fast, efficient new scintillator," *IEEE Trans. Nucl. Sci.*, vol. 39, no. 4, pp. 502–505, 1992.

[5] D. W. Cooke *et al.*, "Crystal growth and optical characterization of cerium-doped $Lu_{1.8}Y_{0.2}SiO_5$," *J. Appl. Phys.*, vol. 88, no. 12, pp. 7360–7362, 2000.

[6] S. Shimuzu *et al.*, "Scintillation properties of $Lu_{0.4}Gd_{1.6}SiO_5 : Ce$ (LGSO) crystal," *IEEE Trans. Nucl. Sci.*, vol. 53, no. 1, pp. 14–17, Feb. 2006.

[7] N. J. Cherepy *et al.*, "Transparent ceramic scintillator fabrication, properties and applications," in *Proc. SPIE—Hard X-Ray, Gamma-Ray, and Neutron Detector Physics X*, San Diego, 2008, vol. 7079, pp. 70790X–70790X-6.

[8] N. J. Cherepy *et al.*, "Comparative gamma spectroscopy with SrI2(EU), GYGAG(Ce) and Bi-Ioaded plastic scintillators," in *Proc. IEEE Nucl. Sci. Symp. (NSS/MIC)*, Knoxville, 2010, pp. 1288–1291.

[9] K. Kamada *et al.*, "2 inch diameter single crystal growth and scintillation properties of $Ce : Gd_3Al_2Ga_3O_{12}$," *J. of Crystal Growth, doi:10.1016/j.jcrysgro.2011.11.085.*, 2012.

[10] D. Renker, "New developments on photosensors for particle physics," *Nucl. Instrum. Meth. A.*, vol. 598, no. 1, pp. 207–212, Jan. 2009.

[11] N. Otte, "The silicon photomultiplier—a new device for high energy physics, astroparticle physics, industrial and medical applications," in *Proc. SNIC Symp.*, Stanford, 2006, pp. 1–9, Paper 18.

[12] E. Grigoriev *et al.*, "Silicon photomultipliers and their bio-medical applications," *Nucl. Instrum. Meth. A.*, vol. 571, no. 1–2, pp. 130–133, Nov. 2007.

[13] V. Bindi, A. D. Guerra, G. Levi, L. Quadrani, and C. Sbarrab, "Preliminary study of silicon photomultipliers for space missions," *Nucl. Instrum. Meth. A.*, vol. 572, no. 2, pp. 662–667, Mar. 2007.

[14] W. W. Moses and S. E. Derenzo, "Prospects for time-of-Flight PET using LSO scintillator," *IEEE Trans. Nucl. Sci.*, vol. 46, no. 3, pp. 474–468, 1999.

[15] V. C. Spanoudaki and C. S. Levin, "Investigating the temporal resolution limits of scintillation detection from pixellated elements: Comparison between experiment and simulation," *Phys. Med. Bio.*, vol. 56, pp. 735–756, 2011.

[16] D. Renker, "Geiger-mode avalanche photodiodes, history, properties and problems," *Nucl. Instrum. Meth. A.*, vol. 567, no. 1, pp. 48–56, Jun. 2006.

[17] A. N. Otte *et al.*, "A test of silicon photomultipliers as readout for PET," *Nucl. Instrum. Meth. A.*, vol. 545, no. 3, pp. 705–715, Apr. 2005.

[18] T. Wilmshurst, *Signal Recovery from Noise in Electronic Instrumentation*. New York: Adam Hilger, 1985.

[19] M. Moszynski, T. Ludziejewski, D. Wolski, W. Klamra, and V. V. Avdejchikov, "Timing properties of GSO, LSO and other Ce doped scintillators," *Nucl. Instrum. Meth. A.*, vol. 372, no. 1–2, pp. 51–58, Mar. 1996.

[20] S. E. Derenzo, W. W. Moses, S. C. Blankespoor, M. Ito, and K. Oba, "Design of a pulsed X-ray system for fluorescent lifetime measurements with a timing resolution of 109 ps," *IEEE Trans. Nucl. Sci.*, vol. 41, no. 3, pp. 629–631, Jun. 1994.

[21] S. E. Derenzo *et al.*, "Design and implementation of a facility for discovering new scintillator materials," *IEEE Trans. Nucl. Sci.*, vol. 55, no. 3, pp. 1458–1563, 2008.

[22] L. M. Bollinger and G. E. Thomas, "Measurement of the time dependence of scintillation intensity by a delayed-coincidence method," *Rev. Sci. Instrum.*, vol. 32, pp. 1044–1050, 1961.

[23] H. Suzuki, T. A. Tombrello, C. L. Melcher, C. A. Peterson, and J. S. Schweitzer, "The role of gadolinium in the scintillation processes of cerium-doped gadolinium oxyorthosilicate," *Nucl. Instrum. Meth. A.*, vol. 346, no. 3, pp. 510–521, Aug. 1994.

[24] R. I. Wiener, S. Surti, C. Piemonte, and J. S. Karp, "Timing and energy characteristics of LaBr3[Ce] and CeBr3 scintillators read by FBK siPMs," in *Proc. IEEE Nucl. Sci. Symp. (NSS/MIC)*, Valencia, Spain, 2011, pp. 4013–4019.

[25] A. Gola, C. Piemonte, and A. Tarolli, "The DLED algorithm for timing measurements on large area SiPMs coupled to scintillators," *IEEE Trans. Nucl. Sci.*, vol. 59, no. 2, pp. 358–365, Apr. 2012.

[26] M. Massimo *et al.*, "Electro-Optical Performances of p-on-n and n-on-p Silicon Photomultipliers," *IEEE Trans. Electron Dev.*, vol. 59, no. 12, pp. 3419–3425, Dec. 2012.

[27] [Online]. Available: www.hamamatsu.com

[28] [Online]. Available: www.advansid.com

[29] H. T. van Dam *et al.*, "A comprehensive model of the response of silicon photomultipliers," *IEEE Trans. Nucl. Sci.*, vol. 57, no. 4, pp. 2254–2266, Aug. 2010.

[30] G.-C. Wang, "Timing optimization of solid-state photomultiplier based PET detectors," *IEEE Trans. Nucl. Sci.*, vol. 57, no. 1, pp. 25–30, Feb. 2010.

[31] S. Yamamoto, J. Y. Yeom, K. Kamada, T. Endo, and C. S. Levin, "Development of an ultrahigh resolution block detector based on 0.4 mm pixel Ce:GAGG scintillators and a silicon photomultiplier," presented at the IEEE Symp. on Radiation Measurements and Applications, Oakland, CA, May 14–17, 2012.

Authorized licensed use limited to: Australian National University. Downloaded on March 12,2020 at 00:31:51 UTC from IEEE Xplore. Restrictions apply.